Abstract

The precipitation legacy effect, defined as the impact of historical precipitation (PPT) on extant ecosystem dynamics, has been recognized as an important driver in shaping the temporal variability of dryland aboveground primary production (ANPP) and soil respiration. How the PPT legacy influences whole ecosystem-level carbon (C) fluxes has rarely been quantitatively assessed, particularly at longer temporal scales. We parameterized a process-based ecosystem model to a semiarid savanna ecosystem in southwestern US, calibrated and evaluated the model performance based on 7 years of eddy covariance measurements, and conducted two sets of simulation experiments to assess interdecadal and interannual PPT legacy effects over a 30-yr simulation period. The results showed that decreasing the previous period/year PPT (dry legacy) always increased subsequent net ecosystem production (NEP) whereas increasing the previous period/year PPT (wet legacy) decreased NEP. The simulated dry legacy impacts mostly increased subsequent gross ecosystem production (GEP) and reduced ecosystem respiration (R_e) but the wet legacy mostly reduced GEP and increased R_e. Although the direction and magnitude of GEP and R_e responses to the simulated dry and wet legacies were influenced by both the previous and current PPT conditions, the NEP responses were predominantly determined by the previous PPT characteristics including rainfall amount, seasonality and event size distribution. Larger PPT difference between periods/years resulted in larger legacy impacts, with dry legacies fostering more C sequestration and wet legacies more C release. The carryover of soil N between periods/years was mainly responsible for the GEP responses while the carryovers of plant biomass, litter and soil organic matter were mainly responsible for the R_e

responses. These simulation results suggest that previous PPT conditions can exert substantial legacy impacts on current ecosystem C balance, which should be taken into account while assessing the response of dryland ecosystem C dynamics to future PPT regime changes.

Keywords: Carbon flux, lagged effect, biogeochemical carryover, ecosystem modeling, legacy, semiarid.

1 Introduction

Drylands play an important role in global carbon (C) cycle and future C sequestration (Houghton et al., 1999; Asner et al., 2003), as they cover 30-45% of the earth's land surface (Asner et al., 2003; Reynolds et al., 2007), store about 15% of the global soil organic carbon (Schlesinger, 1991), and represent 30-35% of terrestrial net primary production (Field et al., 1998). Driven by sporadic precipitation (PPT) and nonlinear biological responses, dryland C fluxes are especially variable across time and space (Maestre et al., 2012; Collins et al., 2014), making the prediction of dryland C budgets a challenging task (Jenerette et al., 2012). Moreover, climate models predict that the intra- and inter-annual PPT variability may be further intensified in dryland regions with longer drought durations and more large-sized events (Solomon et al., 2007; Diffenbaugh et al., 2008; Cook and Seager, 2013). Further, sequences of wet years followed by sequences of dry years and *vice versa* are also increasingly likely (Peters et al., 2012; Sala et al., 2012). Understanding the response of dryland ecosystem C fluxes to PPT variation is, therefore, important to characterizing the global C cycle and predicting how future PPT regime changes will affect dryland C balance.

As a measure of ecosystem C balance, net ecosystem production (NEP) has a value that is positive when an ecosystem accumulates C and negative when an ecosystem loses C. Dryland NEP is closely tied to current-year PPT amount, with wetter than average years being a C sink, drier than average years being a C source, and years with average rainfall being C neutral (Flanagan et al., 2002; Hastings et al., 2005). Additionally, at seasonal scales, the distribution of PPT in addition to the total amount can have large influences on ecosystem production

(Porporato et al., 2004; Katul et al., 2007). At interannual scales a PPT legacy effect, defined as the impact of past PPT conditions on the current structure and functioning of ecosystems (Lauenroth and Sala, 1992; Sala et al., 2012; Monger et al., 2015), has also been found to play an important role in shaping the temporal variability of dryland ecosystem C fluxes (Knapp et al., 2002; Huxman et al., 2004a, b; Heisler and Weltzin, 2006; Sala et al., 2012; Ogle et al., 2014). For example, Hasting et al. (2005) attributed the C sink status of a desert shrub ecosystem in the early spring of 2002 to the above-average rainfall in the late fall of 2001. Scott et al. (2009) and Hamerlynck et al. (2013) found that a cool season (Dec - Apr) drought was followed by an unusually large net C loss during the following warm monsoon season (Jul - Sep) in a semiarid savanna and a semi-desert grassland. Moreover, the savanna ecosystem has recently been a net C source and one hypothesized but untested explanation is due to an increase in current respiration of organic C that accumulated in the preceding wetter decade (Scott et al., 2009). While these studies reveal the existence of PPT legacy effects on NEP at the seasonal scale, only a few studies have quantitatively assessed the contribution of PPT legacy to the temporal variability of dryland NEP at interannual and interdecadal time scales (Williams and Albertson, 2006), mainly because it is methodologically difficult to separate the past and current PPT impacts on C fluxes with the limited observational data (Sala et al., 2012), and there is a general lack of field manipulative experiments to address the PPT legacies at these scales (Reichmann et al., 2013a).

Much of our current understanding of the PPT legacy effects on dryland C fluxes is based on aboveground net primary production (ANPP). A number of studies have documented that

72 dryland ANPP is not only linearly related to current-year PPT, but also closely related to the PPT
73 amount and seasonality several months to years before (Lauenroth and Sala, 1992; Oesterheld et
74 al., 2001; Huxman et al., 2004c). For example, field studies have found a positive legacy
75 impact where ANPP is higher than expected if preceded by a wetter year, or lower than expected
76 if preceded by a drier year (Jobbagy and Sala, 2000; Oesterheld et al., 2001; Wiegand et al., 2004;
77 Sherry et al., 2008; Sala et al., 2012). Proposed mechanisms explaining such observed positive
78 PPT legacy effects on ANPP mainly involve the structural carryovers between years, which can
79 be leaf and root biomass (Oesterheld et al., 2001), the composition of species differing in rooting
80 depth and phenology (Paruelo et al., 1999; Jobbagy and Sala, 2000), or the density of seeds,
81 tillers and plant individuals (Oesterheld et al., 2001; Yahdjian and Sala, 2006; Reichmann et al.,
82 2013a). Alternatively, a negative legacy effect occurs when production is lower than expected
83 if preceded by a wet period or higher than expected if preceded by a dry period (Jenerette et al.,
84 2010). A negative PPT legacy effects may be influenced more by biogeochemical carryovers
85 that influence the resource availability to respond to current PPT (Evans and Burke, 2013;
86 Reichmann et al., 2013b), whereby increased growth in response to a higher PPT can reduce the
87 available nutrients (e.g., nitrogen (N)) for the following period and *vice versa*. Although
88 various mechanisms have been proposed for the PPT legacy impacts on ANPP, few of them have
89 been rigorously tested, and the key underlying mechanisms still remain poorly understood
90 (Sherry et al., 2008; Williams et al., 2009; Sala et al., 2012; Monger et al., 2015).
91 Soil respiration (R_s), as a major component of ecosystem C efflux, has also been found to have
92 lagged responses to PPT variations (Huxman et al., 2004b; Sponseller, 2007; Ma et al., 2012;

93 Cable et al., 2013). This is particularly true at the event scale; after a period of drought, a
94 rainfall event can result in a pulse of CO_2 efflux that may be orders of magnitude larger than that
95 before the event and then decline exponentially for a few days to weeks (Xu et al., 2004;
96 Jenerette et al., 2008; Borken and Matzner, 2009; Cable et al., 2013; Oikawa et al., 2014). At a
97 seasonal scale, Vargas et al. (2010) found no lags between R_s and soil moisture across 13
98 vegetation types including four grasslands; but Hamerlynck et al. (2013) presented longer-term
99 ecosystem flux data that suggest seasonal drought legacies affect ecosystem respiration (R_e) in a
100 semi-desert grassland in southeastern AZ, US. They posited that the increased C substrate
101 availability resulting from the previous cool-season drought induced plant mortality was
102 responsible for the higher R_e in the following monsoon season. However, very few studies have
103 been devoted to understanding the PPT legacy impacts on dryland respiration at greater than
104 seasonal timescales.
105 In this study, we conducted simulation experiments with a widely-used dryland ecosystem
106 model, Patch Arid Land Simulator (PALS; Kemp et al. 1997, 2003; Reynolds et al. 2004; Shen et
107 al. 2009), to analyze the PPT legacy effects on ecosystem-level C fluxes including NEP, gross
108 ecosystem production (GEP), and R_e. The PALS model was built on the pulse-reserve concept
109 (Noy-Meir, 1973) and had been used to analyze the impacts of antecedent moisture conditions
110 and the lagged responses of different plant functional types in three North American deserts at
111 the rainfall event scale (Reynolds et al., 2004). We parameterized, calibrated, and evaluated the
112 model based on the long-term eddy covariance measured fluxes at a semi-desert savanna
113 ecosystem in southwestern US (Scott et al., 2009) to analyze the PPT legacy effects at

114 interannual and interdecadal scales. Specifically, we addressed the following two questions.
115 First, what are the direction and magnitude of ecosystem C flux responses to dry and wet
116 legacies? We expected that the PPT legacy impacts would occur over annual and decadal scales
117 in correspondence to PPT fluctuations at these scales, and the dry and wet legacy impacts would
118 differ in direction and magnitude. Second, how are the direction and magnitude of PPT legacy
119 effects related to the PPT characteristics of both the previous and the current year / period? We
120 expected that greater variability in PPT would lead to corresponding increases in legacy effect.
121 For PPT characteristics, we were not only interested in the annual and seasonal PPT amount but
122 also between-event interval and event size distribution, since these variables are
123 widely-recognized key PPT features to dryland ecosystems (Porporato et al., 2004; Katul et al.,
124 2007; Shen et al., 2008).
125

126 ## 2 Methods

127 ### 2.1 Model description

128 PALS is a process-based ecosystem model that consists of four modules: atmospheric forcing,
129 a water cycling and energy budget, plant production and respiration, and soil organic matter
130 (SOM) decomposition and heterotrophic respiration (R_h). The four modules are interactively
131 linked by the cycling of C, N, and H_2O through the atmosphere-plant-soil continuum. The
132 PALS model explicitly considers seven plant functional types (FTs) commonly found in the
133 North American warm deserts: evergreen shrub, deciduous shrub, perennial forb, perennial C_3
134 and C_4 grasses, and native and exotic C_3 annual grasses (Reynolds et al., 1997; Shen et al., 2009).

135 Since the detailed model structure and mechanistic relationships have been presented in several
136 publications (Kemp et al., 1997, 2003; Reynolds et al., 1997, 2000, 2004; Gao & Reynolds, 2003;
137 Shen et al., 2005, 2008a, 2008b, 2009), here we briefly describe the four modules and refer to the
138 specific literature for detailed description.

139 The atmospheric driving force module reads in data for atmospheric driving variables (e.g.
140 atmospheric [CO_2], N deposition rate, daily maximum and minimum air temperatures, PPT,
141 relative humidity, and solar radiation), and based on these driving variables, calculates other
142 important variables such as vapor pressure deficit (VPD) that determines stomatal conductance
143 and soil temperature that influences SOM decomposition and soil respiration. Calculations of
144 VPD and soil temperature can be found in Equations (2) - (7) in Shen et al. (2005).

145 The water cycling and energy budget module mainly calculates soil water contents at six
146 layers, the rates of water infiltration into and percolation out of a layer, and water losses via
147 evaporation and transpiration from different layers. Water infiltration and percolation rates of a
148 layer are determined by the effective PPT reaching the soil surface, previous water content, and
149 the water holding capacity as a function of soil texture (Shen et al., 2005). Soil evaporation is
150 determined by soil water availability and energy available in the two top soil layers (10 cm in
151 depth). Water uptake by plants is partitioned among the soil layers according to the proportion
152 of roots in each layer for all plant FTs (Kemp et al., 1997; Shen et al., 2008b). Canopy
153 transpiration is calculated by using the energy budget and the canopy stomatal resistance
154 (Reynolds et al., 2000; Gao and Reynolds, 2003).

155 The plant production and respiration module mainly simulates phenology, primary production,

156 growth and maintenance respiration, photosynthate allocation, and litterfall of each plant FT.
157 Three major phenophases (i.e. dates of germination, leafing, and dormancy) are determined in
158 PALS based on the observed dates, air temperature, and PPT (Shen et al., 2009). Primary
159 production for each FT is calculated based on the leaf area, potential net photosynthetic rate,
160 stomatal conductance, leaf N content modifier, and the difference between intercellular and
161 atmospheric [CO_2]. The plant photosynthesis rate is estimated as a product of stomatal
162 conductance and the partial pressure gradient between atmospheric and intercellular [CO_2].
163 The stomatal conductance is calculated as an exponential function of leaf water potential that
164 decreases linearly with atmospheric vapor deficit (see Equations (10) - (14) in Shen et al., 2005).
165 Photosynthate is allocated to different plant organs (leaf, stem, and root) using fixed allocation
166 ratios after subtracting the maintenance respiration, which is estimated as a function of live
167 biomass, basal respiration rate, and modifiers of temperature and plant water potential (Shen et
168 al., 2008a). Growth respiration is calculated based on the growth yield coefficient and the net
169 photosynthate used for growth (Shen et al., 2008a). Litterfall amount is mainly determined as a
170 function of observed dormancy dates, maximum air temperature and drought conditions (Shen et
171 al., 2008a; Shen et al., 2009).
172 The SOM decomposition and heterotrophic respiration module simulates the decomposition of
173 metabolic and structural litter material, SOM in active, slow and passive pools, and CO_2
174 emissions associated with these decomposition processes (Kemp et al., 2003; Shen et al., 2009).
175 The SOM decomposition rate or heterotrophic rate is calculated as a first-order kinetics rate with
176 a decomposition coefficient multiplied by the pool size and the temperature and moisture scalars

177 (see Equations (A4)-(A11) in Shen et al., 2009). In addition, this module also simulates the
178 dynamics of soil mineral N pool by using N mineralization and atmospheric deposition as the
179 major inputs, and plant N uptake and leaching loss as the major outputs. Among these the N
180 mineralization and plant uptake processes are modeled in more detail while the rates of the other
181 processes are basically assigned with empirical constant values. The N mineralization
182 processes are directly coupled to litter and SOM decomposition processes and are calculated as a
183 product of the C flow rates and the C/N ratio of the corresponding litter or SOM pools (Parton et
184 al., 1993; Kemp et al., 2003). The plant N uptake is a product of water transpiration and N
185 concentration in soil solution (see Equation (8) in Shen et al., 2008b).
186
187 **2.2 Model parameterization**
188 For this study, we modified and parameterized PALS to represent an upland mesquite savanna
189 ecosystem in the Santa Rita Experimental Range (SRER; 31.8214^{o} N, 110.8661^{o} W, elevation
190 1116 m), about 45 km south of Tucson, AZ, USA. Soils at this site are a deep sandy loam
191 (Scott et al., 2009), and the mean groundwater depth likely exceeds 100 m (Barron-Gafford et al.,
192 2013). PPT was therefore considered as the only source of water input into the system. Based
193 on the vegetation composition (Scott et al., 2009), there were five major plant FTs included in
194 PALS: shrub (e.g. *Prosopis velutina*), subshrub (e.g. *Isocoma tenuisecta*), C_4 perennial grass (e.g.
195 *Digitaria californica*), perennial forb (e.g. *Ambrosia psilostachya*), and C_3 annual grass, among
196 which the velvet mesquite shrub with average height of ca. 2.5 m accounted for ~35% of the
197 total canopy cover and other FTs (mainly perennial grasses) accounted for ~22% (Scott et al.,

198 2009). Therefore, we derived the site-characteristic parameters for the two major FTs (shrub
199 and perennial grass) from previous studies carried out in SRER, with those for the other FTs
200 being adopted from a generic parameter dataset for the PALS model to be used in the North
201 American warm deserts (Reynolds et al., 2004; Shen et al., 2005). These site-specific
202 parameters mainly included plant-related parameters (e.g. canopy cover, C allocation ratio,
203 rooting distribution ratio, and the initial values of living and dead plant biomass pools) and
204 soil-related parameters (e.g. soil chemical and physical properties, C/N ratios, decomposition
205 rates, and initial values of the litter and SOM pools). The values of these parameters are
206 provided in Supplementary Table S1, with cited literature also being listed below the table.
207 For the climatic variables used to drive the PALS model, we compiled a 30-year
208 meteorological dataset that included daily PPT, maximum and minimum air temperatures (T_{max}
209 and T_{min}), relative humidity (RH), and total solar radiation (S_{rad}) from 1981 to 2010. The T_{max},
210 T_{min}, RH, and S_{rad} data from 1981-1990 were observations from the Tucson weather station
211 (about 50 km north of the mesquite savanna site and lower elevation) and obtained through the
212 Arizona Meteorological Network online data access (AZMET: http://ag.arizona.edu/azmet).
213 The remaining 20 years (1991-2010) of T_{max}, T_{min}, RH and S_{rad} data were observations from the
214 Kendall Grassland meteorologial site (about 85 km east of the mesquite savanna site and slightly
215 higher elevation) and obtained through the Southwest Watershed Research Center (SWRC)
216 online data access (http://www.tucson.ars.ag.gov/dap/). The 30-year PPT data were
217 observations from the Santa Rita Watershed rain gage #5 (1.5 km from the site) and obtained
218 also from the SWRC online data access. These different sources of meteorological data were

219 adjusted based on the 7 years (2004-2010) of the meteorological data obtained from the
220 AmeriFlux eddy-covariance flux tower at the mesquite savanna site (US-SRM, see
221 Supplementary Fig. S1). At last, we used the AZMET and SWRC data from 1981 to 2003 plus
222 the flux tower data from 2004 to 2010 to drive the model.
223 Since our simulation experiment was based on the manipulations of the 30-year (1981-2010)
224 PPT data, we report the PPT characteristics here in more detail. In the past 30 years, the mean
225 annual PPT (MAP) amount was 401 mm at the site, slightly greater than the long-term
226 (1937-2007) mean of 377 mm (Scott et al., 2009). These 30 years were divided into two
227 periods: a wet period from 1981-1994 with a MAP of 449 mm and a dry period from 1995 to
228 2010 with a MAP of 347 mm (Fig. 1a). For the analysis of PPT legacy effects at interdecadal
229 scale, the wet period was treated as the previous period and the dry period as the current period.
230 For the analysis of PPT legacy effects at interannual scale, the annual scale was defined as from
231 July through June of the next year. To analyze the relationship between PPT legacy effects and
232 seasonal rainfall characteristics, each year was further divided into four seasons (with their mean
233 rainfall in parentheses): the main warm growing season from July to September (warm-GS, 224
234 mm), the cool dry season from October to November (cool-DS, 48 mm), the minor cool growing
235 season from December to March (cool-GS, 104 mm), and the warm dry season from April to
236 June (warm-DS, 26 mm). At the site, as in many other dryland regions (Sala et al., 1992;
237 Heisler-White et al., 2008), most rainy days have only light rainfall events. About 80 % of
238 daily rainfall was < 10 mm, with medium- to large-sized events (10 - 50 mm) accounting for
239 about 20% and only 10 events larger than 50 mm in the 30 years (Fig. 1b). The no-rain-day

240 duration between events (hereafter between-event interval or BEI) was ~5 days on average in the
241 warm-GS and ~10 days in the cool-GS (Fig. 1c). The average BEI was ~17 days in the cool-DS
242 and 24 days in the warm-DS; but there could be no rain for three months in these dry seasons
243 (Fig. 1c).
244
245 **2.3 Model calibration and evaluation**
246 After model parameterization, we calibrated the model based on four years (2004-2007) of
247 CO_2 and H_2O flux data monitored using the eddy covariance technique at the savanna site.
248 Detailed descriptions of instrumentation, sensor heights and orientations, and data processing
249 procedures for the eddy covariance data can be found in Scott et al. (2009). During model
250 calibration, we mainly adjusted the parameter values of photosynthate allocation ratios, live
251 biomass death rates, and SOM decomposition rates to achieve a best fit between modeled and
252 observed GEP and R_e, since these parameters have been identified as the most sensitive and
253 uncertain ones (e.g. photosynthate allocation ratios) in influencing the modeled ecosystem
254 carbon fluxes (Shen et al., 2005). The model performed well in capturing the seasonal variation
255 patterns of actual evapotranspiration (AET), GEP, R_e, and NEP in the four calibration years
256 (Supplementary Fig. S2), with larger C fluxes during the warm-GS than in the other seasons.
257 At the annual scale, simulated AET, GEP, and R_e explained over 60% of the variations in the
258 observations (Fig. 2, left panels), but the correlation between the simulated and observed NEP
259 was very weak (Fig. 2d). This was mainly because the model substantially overestimated GEP
260 (120 g C m^{-2} simulated *versus* 52 g C m^{-2} observed) in the cool-GS of 2006 (Supplementary Fig.

S3b). Further explanations on the possible causes of the GEP overestimation in 2006 shall be provided latter in discussion. If the data of this year were excluded, the explanatory power for annual NEP could reach 74%. Since our goal was to use an empirically plausible model to understand the long-term temporal variations in ecosystem fluxes, we consider the calibration results acceptable.

The model performance was further evaluated by assessing the degree of correlation between the PALS-simulated and flux-tower-measured C and H_2O fluxes from 2008 through 2010, which were not used for model calibration. The coefficients of determination (R^2), which describe the proportion of the variance in measured data explained by the model, were all larger than 0.9 in the three validation years (2008-2010; Fig. 2, left panels). These evaluation results indicate that the model was capable of capturing the temporal variability of observed fluxes at the annual scale. Furthermore, we also analyzed the relationships between the observed and simulated fluxes with the corresponding current-year PPT to see how the flux variations were explained by current-year PPT under baseline conditions (i.e. the PPT variations shown in Fig. 1). The explanatory power (R^2) for both the observed and simulated fluxes were mostly over 70% (Fig. 2, right panels), which further indicates that the model is capable of capturing the impacts of PPT variability on ecosystem fluxes. The following simulation experiments were therefore designed to discriminate the contributions by previous- and current-year PPT impacts.

2.4 Simulation experiments

We designed two sets of simulation experiments to examine the interdecadal and interannual

PPT legacy effects. To analyze the interdecadal legacy effects, we first changed the PPT of the 14-year previous period (1981-1994) by 0%, ±10%, ±30%, ±50% and ±80% (multipliers of existing daily PPT amounts in the record) while keeping the 16-year current-period (1995-2010) PPT unchanged. After these manipulations, the average PPT of the previous period ranged from 93 mm corresponding to the 80% of decrease to 837 mm corresponding to the 80% of increase. This design detects how changes in previous-period PPT influence the current-period C fluxes and the associated C pool dynamics. On top of each previous period PPT manipulation level, we further changed the current-period PPT by 0%, ±10%, ±30%, ±50%, and ±80%, which resulted in the average current-period PPT varying from 69 mm to 621 mm. This design detects how changes in the current-period PPT influence the legacies resulting from changes in the previous-period PPT. As a result, we conducted 73 simulation runs corresponding to the 73 combinations of the above previous- and current-period PPT manipulations (9 previous PPT levels times 8 current PPT levels plus 1 baseline run).

To analyze the interannual legacy, we changed the PPT of each individual year by ±30% while keeping the PPT of the subsequent years unchanged. This design resulted in 54 simulation runs (27 years from 1981-2007 times 2 PPT manipulation levels) and illustrates the effects of changes in the PPT of the previous one year on the C fluxes and resource pools of the current year(s). After a 30% of PPT change, annual PPT ranged from 162 mm to 925 mm in the 27 years, which was large enough to cover the PPT interannual variation at the study site. Another consideration of using 30% as the PPT manipulation level was that future projected annual PPT variation in dryland regions will be -30% to +25% (Bates et al., 2008; Maestre et al.,

303 2012).

304

305 **2.5 Data analysis**

306 Legacy effect was quantified as the C flux (or resource pool size) of the current-period/year
307 after PPT changes in the previous-period/year minus that without PPT changes in the
308 previous-period/year. As an example, the following equation calculates the legacy effect of
309 increasing the previous-period PPT by 30% on the current-period NEP:

310 $$Legacy_{NEP} = \Delta NEP = NEP^{CP}_{PPT+30\%} - NEP^{CP}_{PPT+0\%}$$

311 where $NEP^{CP}_{PPT+30\%}$ is the cumulative NEP throughout the current period (1995-2010) under a
312 30% of previous-period (1981-1994) PPT increase; $NEP^{CP}_{PPT+0\%}$ is the cumulative NEP
313 throughout the current period with no previous-period PPT change (i.e. the baseline PPT
314 conditions shown in Fig. 1). This method directly quantifies whether changes in PPT of the
315 previous period will impose a positive, negative, or no legacy effect on the C fluxes (or resource
316 pools) of the current period. For simplicity, hereafter we refer to the legacy effect resulting
317 from the decreased previous-period/year PPT as the dry legacy and that resulting from the
318 increased previous-period/year PPT as the wet legacy. Spearman correlation analysis was used
319 to detect the relationships between legacy effects and PPT characteristics, including PPT amount,
320 BEI, and the number of large (≥10 mm) *versus* small (<10 mm) events at yearly and seasonal
321 scales. The correlation analysis was performed in SPSS 16.0 (Chicago, IL, USA).

3 Results

3.1 Interdecadal legacy

Changes in PPT of the previous period (1981-1994) imposed obvious legacy impacts on the C fluxes of the current period (1995-2010). The direction of the simulated interdecadal dry and wet legacies on GEP and R_e was dependent upon the direction of both the previous- and current-period PPT changes. When the current-period PPT was reduced (Fig. 3, left panels), the simulated dry legacies mostly increased the current-period GEP (Fig. 3a) but decreased R_e (Fig. 3c); whereas wet legacies imposed little impacts on the current-period GEP (Fig. 3a) but mostly increased R_e (Fig. 3c). When the current-period PPT was enhanced (Fig. 3, right panels), both the dry and wet legacies mostly increased GEP and R_e (Fig. 3b, d). Regardless of current-period PPT changes, NEP always increased with dry legacies and decreased with wet legacies (Fig. 3e, f), indicating a consistent negative NEP response to PPT legacies.

The simulated absolute magnitude of the PPT legacy influence on ecosystem C fluxes (i.e. GEP, R_e, and NEP) generally increased with the absolute magnitude of changes in the previous-period PPT (Fig. 3, Fig. 4). Increasing the current-period PPT generally amplified the legacy effects compared to decreasing the current-period PPT (comparing the left to the right panels of Fig. 3). The magnitude of the PPT legacies was also significantly correlated with the PPT difference between the current and previous period (ΔPPT, equals to the current-period PPT minus the previous-period PPT; Fig. 4). If the previous period was wetter than the current period (i.e. $\Delta PPT < 0$ or a wet-to-dry period transition), the legacy effect on R_e was negatively

342 related with ΔPPT (Fig. 4c) but that on NEP was positively related with ΔPPT (Fig. 4e),
343 indicating more current-period C release after a wetter previous period. In contrast, if the
344 previous period was drier than the current period (i.e. ΔPPT > 0 or a dry-to-wet period
345 transition), the correlations were all positive for GEP, R_e and NEP (Fig. 4, right panels),
346 indicating more current period C sequestration after a drier previous period.
347 The resource pool dynamics were also shaped by the alterations in the previous- and
348 current-period PPTs. We only showed the 30% decrease and increase in the previous- and
349 current-period PPT (i.e. 4 out of 72 pairs of PPT change combinations) as representative
350 examples in Fig. 5, because the major response patterns for the other paired combinations were
351 similar. The duration of the PPT legacy impacts generally lasted for about 6-8 years for plant
352 biomass, litter mass and soil water content (SWC), but much longer for soil organic matter
353 (SOM) and soil mineral N (N_{soil}) (Fig. 5). Based on the resource pool responses in the early 1-2
354 years (i.e. 1995 and 1996) of the current period, the dry legacies decreased biomass, litter and
355 SOM (Fig. 5a-f), but positively impacted N_{soil} (Fig. 5g-h). Contrastingly, the wet legacies
356 increased biomass, litter and SOM (Fig. 5a-f), but negatively impacted N_{soil} (Fig. 5g-h). Similar
357 to the influences on C fluxes, increasing the current-period PPT (Fig. 5, right panels) amplified
358 the PPT legacy impacts on biomass and litter (Fig. 5a-d), and hastened the recovery rates of
359 SOM and N_{soil} to their baseline levels (Fig. 5e-h).
360
361 **3.2 Interannual legacy**
362 At the interannual scale, a 30% decrease or increase in PPT could have legacy impacts on

363 ecosystem C cycling lasting for 2-12 years (Fig. 6a-b). Notably, the direction of GEP and R_e
364 responses to decreasing or increasing previous-year PPT could be positive or negative (Fig. 6c-f).
365 The dry or wet legacy effects on these two fluxes were variable, idiosyncratic, and, in some cases,
366 large at this timescale. However, the simulated dry legacies mostly increased NEP (Fig. 6g)
367 whereas the simulated wet legacies mostly decreased NEP (Fig. 6h), which was similar to legacy
368 responses at the interdecadal scale (Fig. 3e-f).
369 The correlation analysis showed that not only rainfall amount but also BEI and event size
370 distribution could influence the magnitude of the simulated dry and wet legacies (Table 1). The
371 warm-GS PPT of a previous-year was significantly correlated with the dry legacies for NEP and
372 the wet legacies for GEP and NEP (Table 1). On the other hand, the cool-GS PPT of a
373 current-year influenced the dry and wet legacies for C fluxes, but not all of them were
374 statistically significant (Table 1). These results indicate that the legacies were mainly generated
375 in the warm-GS of a previous year, but the current-year cool-GS PPT conditions could influence
376 the C flux responses to the previous-year legacies. Unlike at the interdecadal scale (Fig. 4), our
377 correlation analysis showed that only the dry legacies for NEP had significant correlations with
378 the PPT difference (ΔPPT) between two consecutive years or cool-GSs (Table 1), indicating that
379 the larger the PPT difference between a previous dry year and a current wet year, the greater the
380 legacy impacts on NEP imposed by the previous dry year.
381 To analyze the interannual PPT legacy impacts on the dynamics of resource pools (i.e.
382 biomass, litter, SOM, N_{soil}, and SWC), two wet years (1983 and 1994) and two dry years (1986
383 and 1995) were chosen as examples (see Fig. 1a). The simulated dry legacies reduced biomass,

litter and SOM, but increased N_{soil} and SWC in the first current year (Fig. 7). In contrast, the simulated wet legacies imposed the opposite direction of impacts on the five resource pools (Fig. 7). The simulated PPT legacy impacts on the resource pools could also last for several years, and the direction and magnitude of the legacy impacts in the following years could differ from those in the first year as described above. For example, increasing the PPT of 1995 by 30% caused a positive legacy impact on the biomass of the first following year (i.e. 1996; Fig. 7b) but it became negative in the latter following years (e.g. in 1998; Fig. 7b), further indicating that current-year PPT conditions can influence the direction and magnitude of previous-year PPT legacies.

4 Discussion

4.1 Direction and magnitude of the simulated PPT legacies

Through this simulation analysis we demonstrated that previous PPT could impose substantial legacy impacts on current ecosystem C fluxes at interannual and interdecadal timescales. Notably, our simulation results support the hypothesis proposed for our study site (Scott et al. 2009) that the accumulated SOM during the previous-wet period contributed to the net C release from the ecosystem during the current dry period. This specific test illustrates a major finding from our simulation study of a negative PPT legacy effect on NEP, i.e. decreasing previous PPT increased current NEP whereas increasing previous PPT decreased current NEP (Fig. 3, Fig. 6). Increasing prior PPT (wet legacy) led to limited changes in GEP but consistently increased R_e. Decreasing prior PPT (dry legacy) led to more variable effects for both GEP and R_e that were

405 strongly conditioned on current period PPT such that increasing current PPT was associated with
406 increases in the dry legacy effect. Overall, the effects on GEP were larger than Re for reduced
407 prior PPT and smaller for increased prior PPT, which resulted in a consistent negative PPT
408 legacy on NEP regardless of current PPT. The complexity in the legacy effects on ecosystem C
409 cycling we show here are in part influenced by the contrasting PPT legacy responses of C uptake
410 and emission and their distinct interactions with current PPT distributions.

411 In projecting future dryland C dynamics, the effects of PPT legacies increase the complexity
412 of ecosystem responses to PPT variability. One consistent interaction between legacy and
413 current PPT effects was that larger between-period PPT differences could result in larger legacy
414 effects (Fig. 4), which is in agreement with what have been found in some field studies. For
415 example, the magnitude of drought legacy on ANPP is proportional to the severity of the drought
416 (Yahdjian and Sala, 2006; Swemmer et al., 2007), and dry- or wet-year legacies on ANPP are
417 linearly related to the PPT difference between years (Sala et al., 2012; Reichmann et al., 2013a).
418 Our simulation analysis detected that not only annual PPT amount but also finer scale PPT
419 characteristics such as GS-rainfall, BEI, and event size could be important in determining the
420 interannual-scale PPT legacy effects (Table 1). These simulation results suggest that PPT
421 legacy effects may play a more important role in shaping the temporal variability of dryland
422 ecosystem C fluxes under the projected increase in future PPT variability (Solomon et al., 2007;
423 Cook and Seager, 2013) but that their characterization remains a challenge.

424 The influence of PPT legacies to dryland ecosystem C balance may strongly interact with
425 other sources of variability in dryland C balance including current year PPT (Flanagan et al.,

426 2002; Hastings et al., 2005), growing season length (Xu and Baldocchi, 2004; Ma et al., 2007),
427 seasonal drought (Scott et al., 2009; Scott et al., 2010; Hamerlynck et al., 2013), and other
428 factors such as temperature and vegetation composition (Hui et al., 2003; Hamerlynck et al.,
429 2010; Barron-Gafford et al., 2012; Scott et al., 2014). These interactions are shown by several
430 examples from our simulations. While PPT was wetter than normal in 1987 (537 mm), the NEP
431 was -85 g C m^{-2} yr^{-1} (a C source), due to the negative wet legacy impacts on NEP from several
432 previous wet years before (1982-1985; see Fig. 6h). PPT was nearly normal in 2008 (402 mm),
433 but the simulated NEP was 80 g C m^{-2} yr^{-1} (a C sink), due to the positive dry legacy impacts on
434 NEP from several previous dry years (2002-2007; see Fig. 6g). Our findings of substantial PPT
435 legacy effects are consistent with a recent analysis of 14 years (1997-2011) of eddy covariance
436 measurements, where Zielis et al. (2014) reported that inclusion of previous year's weather (PPT
437 and temperature) into the linear predicting models for NEP increased the explained variance to
438 53% compared to 20% without accounting for previous year's weather, indicating that previous
439 year's weather also played an important role in determining the C balance of the Switzerland
440 subalpine spruce forest. Although response patterns generated from this simulation study
441 compared well with previous field observations, there exists no field study that, to our
442 knowledge, provides a similarly comprehensive analysis of PPT legacies. The simulation
443 experimental design of this study provides helpful insights into designing field manipulative
444 experiments to further test the modeled patterns by focusing on contrasting wet and dry legacies,
445 separating ecosystem production and decomposition, and exploring the difference in prior and
446 current PPT on the magnitude of the PPT legacy effect.

447

448 **4.2 Potential mechanisms of the modeled PPT legacies**

449 There are three basic mechanisms explaining why PPT legacy impacts can occur in a model
450 system like PALS. First, the rate of C fluxes is a function of not only various environmental
451 factors (e.g. PPT and temperature) but also the pool size itself. For example, soil heterotrophic
452 CO_2 efflux (R_h) rate is a product of the decomposition coefficient, two scalar functions
453 accounting for temperature and moisture influences, and also the size of the SOM pool (Kemp et
454 al., 2003; Shen et al., 2009). Change in the SOM pool size from previous PPT thereby affects
455 current R_h. Second, different C pools have different turnover rates that determine whether
456 biogeochemical materials (e.g. biomass or SOM) can be carried over. If the material produced
457 in a previous year has a turnover rate less than one year, it would not be carried over to the next
458 year to form a legacy impact as explained in the first mechanism. In addition, the turnover rates
459 of different C pools also determine legacy duration. For example, SOM pools in the model
460 have relatively slower turnover rates than biomass pools (Shen et al., 2005; Shen et al., 2008b),
461 thus resulting in the longer-lasting legacy impacts on SOM than on biomass or litter pools (Fig. 5
462 and Fig. 7). Third, the interactions between C fluxes and resource (e.g. N or water) availability
463 also determine the direction and magnitude of legacy effects. For example, N carryover as a
464 legacy of a prior dry period (Fig. 5g, h) can impose impacts on the current-period GEP only
465 when the current-period PPT is not so limiting (Fig. 3b). These are the general mechanisms
466 explaining the occurrence of the modeled PPT legacies from a systems perspective. Below we
467 discuss more specifically the major patterns and the responsible biogeochemical carryovers

found in this study.

An intuitive first explanation for the simulated wet legacies would be the carryover of water. However, in most cases soil water carryover did not occur because the wet legacies on SWC were mostly negative or close to zero at the beginning of the current period/year (Fig. 5i-j; Fig. 7i-j). Soil water carryover was therefore not the major contributor to the modeled PPT legacy effects at interdecadal and interannual scales. This simulation result corroborates with field studies that have shown that carryover of water across long temporal scales is rare in dryland ecosystems, because the rainy growing seasons or wet years are often separated by dry dormant seasons or dry years resulting in short residence times (Oesterheld et al., 2001; Reichmann et al., 2013a; Scott et al., 2014).

The carryover of soil N (N_{soil}) is mainly responsible for the modeled GEP responses. In the PALS model, the photosynthetic rate is linearly related to N availability if plant N demand is not fulfilled (Reynolds et al., 2004; Shen et al., 2005). Therefore, the enhanced N_{soil} from dry legacies (Fig. 5g, h and Fig. 7g, h) generated mostly positive responses of GEP (Fig.3a, b and Fig. 6c). The simulated dry legacies increased N_{soil} mainly through suppressed plant growth (e.g. the reduced biomass and litter production shown in Fig. 5 and Fig. 7) that limited N uptake, which is consistent with many field measurements that N_{soil} accumulates under drought conditions (Reynolds et al., 1999; Yahdjian et al., 2006; Yahdjian and Sala, 2010; de Vries et al., 2012; Evans and Burke, 2013; Reichmann et al., 2013b). Although diverse mechanisms of inorganic N accumulation during dry periods have been proposed in field studies, such as the diffusion restriction of N ions in thin water films of dry soil, the reduced N immobilization by

489 microbial growth and plant uptake, and the reduced N loss from the soil via leaching (Yahdjian et
490 al., 2006), our simulation results suggest that reduced plant uptake may be the main contributor
491 to the N_{soil} accumulation during dry periods. Given the accumulated N_{soil} as a dry legacy, how
492 ecosystem C fluxes such as GEP respond to this dry legacy may be influenced by current PPT
493 conditions. If current PPT conditions were favorable (e.g. the increasing current-period PPT
494 treatment shown in Fig. 3b and the relatively wet years shown in Fig. 6c), GEP mostly increased
495 with a dry legacy (or the accumulated N) because both N and H_2O availabilities were favorable
496 for plant growth (or GEP). Contrastingly, if current PPT conditions were unfavorable (e.g. the
497 decreasing current-period PPT treatment shown in Fig 3a and the relatively dry years shown in
498 Fig. 6c), the GEP responses could be reduced because of the constrained plant growth and the
499 reduced biomass in previous dry years (see Fig. 5c and Fig. 7b).
500 Similarly, the mostly negative responses of GEP to wet legacies (see Fig. 3a, b and Fig. 6d)
501 can be explained by the reduced N_{soil} (Fig. 5g, h and Fig. 7g, h). The decrease of N_{soil} with
502 increasing PPT in the PALS model is mainly attributed to the increases in plant N uptake and the
503 N leaching loss that is calculated as a linear function of PPT amount (Shen et al., 2005).
504 Similar to our simulation results, several field studies found that N uptake increases and N_{soil}
505 decreases under wet conditions in dryland ecosystems (McCulley et al., 2009; McCalley and
506 Sparks, 2009; Yahdjian and Sala, 2010; Reichmann et al., 2013b). However, contrary to our
507 model assumption that N leaching loss is greater in wet than in dry years, some recent field
508 studies reported that the N leaching loss actually is higher in dry than in wet years or at wet sites
509 (McCulley et al., 2009; Evans et al., 2013; Reichmann et al., 2013b; Homyak et al., 2014),

510 resulting in a more "open" N cycle under drier conditions. If these recent field study results are
511 also true for our semi-desert savanna ecosystem, the model assumption could potentially cause
512 an overestimation of N_{soil} carryover effects as shown in Fig. 3 and Fig. 6. Further studies are
513 needed to discriminate the relative contributions of different N processes (e.g. plant uptake,
514 microbial immobilization and mineralization, denitrification, ammonia volatilization, and
515 leaching) to the dynamics of soil inorganic N pools. Nevertheless, this simulation analysis
516 highlights the importance of interactions between N and H_2O availabilities in creating the legacy
517 impacts of PPT and in shaping the temporal variability of dryland ecosystem C fluxes.
518 The carryover of organic material (biomass, litter and SOM) is mainly responsible for the
519 modeled R_e responses. In the PALS model, the autotrophic (R_a) and heterotrophic (R_h)
520 respiration rates are linearly related to the size of biomass, litter and SOM pools (Kemp et al.,
521 2003; Shen et al., 2008a; Shen et al., 2009). The previous wet condition benefited biomass,
522 litter and SOM accumulation (Fig. 5 and Fig. 7) which resulted in the mostly positive wet legacy
523 impacts on R_e (Fig. 3c, d and Fig. 6f). Conversely, the dry legacy decreased these pools (Fig. 5
524 and Fig. 7) and therefore resulted in the mostly negative dry legacy impacts on R_e (Fig. 3c, d and
525 Fig. 6e). Contrary to our simulation results that dry legacies are mostly negative on SOM and
526 R_h, some field studies suggest that the labile C resulting from litter decomposition in a dry
527 season may stimulate R_h in the following wet season (Jenerette et al., 2008; Scott et al., 2009;
528 Ma et al., 2012). This is likely because the labile soil C pool in the PALS model only accounts
529 for ~3% of the total SOM and has a very short residence time (1.7 year; see Supplementary Table
530 S1); small amount of seasonal labile C carryover therefore may not exert obvious legacy impacts

on the total SOM pool size and R_h across interannual and interdecadal scales. These results imply that the PPT legacy effects differ in direction and magnitude, depending on the type of C fluxes under consideration, the type of legacies (i.e. dry vs wet), and the temporal scale of analysis.

Several lines of future research will likely be needed to continue improving the understanding of ecosystem legacy dynamics. Structural shifts in vegetation composition such as woody plant encroachment (Potts et al., 2008; Scott et al., 2014), exotic species invasion (Hamerlynck et al., 2010; Scott et al., 2010), and changes in microbial communities (de Vries et al., 2012; Evans and Wallenstein, 2012; Collins et al., 2014), may also interact with the biogeochemical processes to shape the PPT legacy effects on the temporal variability of dryland C fluxes. Furthermore, we need to better understand the legacy effects of extreme events such as the cool-GS drought in 2006 (see Fig. 1a) so that these important events can be adequately simulated. This cool-GS drought may have caused increased plant mortality as reported for a semi-desert grassland nearby our study site (Scott et al., 2010; Hamerlynck et al., 2013), but that is poorly represented in the model and may have caused the overestimation of the modeled GEP in comparison with the observation (see Supplementary Fig. S3b). Finally, our approach that uses a highly resolved process model provides information complementary to contrasting analytical approaches that evaluate ecosystem responses to statistical rainfall regimes (Rodrigo-Iturbe et al., 2006; Katul et al., 2007; Porporato et al., 2013). Improvement of these alternative modeling approaches is needed to both understand general and specific ecosystem responses to changing PPT regimes at temporal scales from events to decades.

5 Conclusions

We learned through this simulation analysis that: 1) previous PPT conditions can impose substantial legacy impacts on the C balance of dryland ecosystems, with dry legacies fostering more current C sequestration and wet legacies causing more current C release; 2) the responses of ecosystem C fluxes to the simulated dry and wet legacies are mostly opposite in direction and asymmetrical in magnitude, with dry legacies being greater for GEP than for R_e and wet legacies being greater for R_e than for GEP; 3) the carryover of N_{soil} is mainly responsible for the GEP responses, and the carryovers of biomass, litter and SOM are mainly responsible for the R_e responses; and 4) the simulated PPT legacy effects can last for several years even with a one-year PPT change and therefore the direction and magnitude of interannual PPT legacy effects are less predictable than interdecadal ones. These simulation results suggest that dryland ecosystems such as these in southwestern US may emit more C that was sequestered in the past into the atmosphere with the predicted drying trend in the region (Seager et al., 2007; Solomon et al., 2007). The temporal variability of ecosystem C fluxes may be further intensified in the region due to the increasing PPT variability and the associated legacy impacts.

Acknowledgements

We thank the USDA-Agricultural Research Service (ARS), Southwest Watershed Research Center (SWRC) and the Arizona Meteorological Network (AZMET) for making their meteorological data open to access. WS acknowledges the financial supports from the Natural Science Foundation of China (31130011, 31425005 and 31290222), the Major State Basic

573 Research Development Program (973 Planning Program 2011CB403206), and the Natural
574 Science Foundation of Guangdong Province, China (S2012020011084). Partial funding for the
575 Santa Rita Mesquite Savanna eddy covariance site is provided by the U.S. Department of Energy
576 AmeriFlux Office (grant DE-AC02-05CH11231).
577

578 **References**

579 Asner, G. P., Archer, S., Hughes, R. F., Ansley, R. J., and Wessman, C. A.: Net changes in
580 regional woody vegetation cover and carbon storage in Texas Drylands, 1937-1999, Global
581 Change Biol., 9, 316-335, 2003.

582 Barron-Gafford, G. A., Scott, R. L., Jenerette, G. D., Hamerlynck, E. P., and Huxman, T. E.:
583 Landscape and environmental controls over leaf and ecosystem carbon dioxide fluxes under
584 woody plant expansion, J. Ecol., 101, 1471-1483, 2013.

585 Barron-Gafford, G. A., Scott, R. L., Jenerette, G. D., Hamerlynck, E. P., and Huxman, T. E.:
586 Temperature and precipitation controls over leaf- and ecosystem-level CO_2 flux along a
587 woody plant encroachment gradient, Global Change Biol., 18, 1389-1400, 2012.

588 Bates, B. C., Kundzewicz, Z. W., Wu, S., and Palutikof, J. P. (Eds.): Climate Change and Water.
589 Technical Paper of the Intergovernmental Panel on Climate Change, IPCC Secretariat,
590 Genenva, 2008.

591 Borken, W. and Matzner, E.: Reappraisal of drying and wetting effects on C and N
592 mineralization and fluxes in soils, Global Change Biol., 15, 808-824, 2009.

593 Cable, J. M., Ogle, K., Barron-Gafford, G. A., Bentley, L. P., Cable, W. L., Scott, R. L., Williams,
594 D. G., and Huxman, T. E.: Antecedent conditions influence soil respiration differences in
595 shrub and grass patches, Ecosystems, 16, 1230-1247, 2013.

596 Collins, S. L., Belnap, J., Grimm, N. B., Rudgers, J. A., Dahm, C. N., D'Odorico, P., Litvak, M.,
597 Natvig, D. O., Peters, D. C., Pockman, W. T., Sinsabaugh, R. L., and Wolf, B. O.: A
598 multiscale, hierarchical model of pulse dynamics in arid-land ecosystems, Annu. Rev. Ecol.

599 Evol. S., 45, 397-419, 2014.
600 Cook, B. I. and Seager, R.: The response of the North American Monsoon to increased
601 greenhouse gas forcing, J. Geophys. Res. Atmos., 118, 1690-1699, 2013.
602 de Vries, F. T., Liiri, M. E., Bjornlund, L., Setala, H. M., Christensen, S., and Bardgett, R. D.:
603 Legacy effects of drought on plant growth and the soil food web, Oecologia, 170, 821-833,
604 2012.
605 Diffenbaugh, N. S., Giorgi, F., and Pal, J. S.: Climate change hotspots in the United States,
606 Geophys. Res. Lett., 35, l16709, doi: 16710.11029/12008GL035075, 2008.
607 Evans, S. E. and Burke, I. C.: Carbon and nitrogen decoupling under an 11-year drought in the
608 shortgrass steppe, Ecosystems, 16, 20-33, 2013.
609 Evans, S. E. and Wallenstein, M. D.: Soil microbial community response to drying and rewetting
610 stress: does historical precipitation regime matter?, Biogeochemistry, 109, 101-116, 2012.
611 Field, C. B., Behrenfeld, M. J., Randerson, J. T., and Falkowski, P.: Primary production of the
612 biosphere: Integrating terrestrial and oceanic components, Science, 281, 237-240, 1998.
613 Flanagan, L. B., Wever, L. A., and Carlson, P. J.: Seasonal and interannual variation in carbon
614 dioxide exchange and carbon balance in a northern temperate grassland, Global Change
615 Biol., 8, 599-615, 2002.
616 Gao, Q. and Reynolds, J. F.: Historical shrub-grass transitions in the northern Chihuahuan Desert:
617 modeling the effects of shifting rainfall seasonality and event size over a landscape gradient,
618 Global Change Biol., 9, 1475-1493, 2003.
619 Hamerlynck, E. P., Scott, R. L., and Barron-Gafford, G. A.: Consequences of cool-season

620 drought-induced plant mortality to Chihuahuan Desert grassland ecosystem and soil
621 respiration dynamics, Ecosystems, 16, 1178-1191, 2013.
622 Hamerlynck, E. P., Scott, R. L., Moran, M. S., Keefer, T. O., and Huxman, T. E.: Growing season
623 ecosystem and leaf-level gas exchange of an exotic and native semiarid bunchgrass,
624 Oecologia, 163, 561-570, 2010.
625 Hastings, S. J., Oechel, W. C., and Muhlia-Melo, A.: Diurnal, seasonal and annual variation in
626 the net ecosystem CO_2 exchange of a desert shrub community (Sarcocaulescent) in Baja
627 California, Mexico, Global Change Biol., 11, 927-939, 2005.
628 Heisler-White, J. L., Knapp, A. K., and Kelly, E. F.: Increasing precipitation event size increases
629 aboveground net primary productivity in a semi-arid grassland, Oecologia, 158, 129-140,
630 2008.
631 Heisler, J. L. and Weltzin, J. F.: Variability matters: towards a perspective on the influence of
632 precipitation on terrestrial ecosystems, New Phytol., 172, 189-192, 2006.
633 Homyak, P. M., Sickman, J. O. , Miller, A. E., Melack, J. M., Meixner, T., and Schimel, J. P.:
634 Assessing nitrogen-saturation in a seasonally dry Chaparral watershed: Limitations of
635 traditional indicators of N-saturation, Ecosystems, 17, 1286-1305, 2014.
636 Houghton, R. A., Hackler, J. L., and Lawrence, K. T.: The US carbon budget: Contributions from
637 land-use change, Science, 285, 574-578, 1999.
638 Hui, D. F., Luo, Y. Q., and Katul, G.: Partitioning interannual variability in net ecosystem
639 exchange into climatic variability and functional change, Tree Physiol., 23, 433-442, 2003.
640 Huxman, T. E., Cable, J. M., Ignace, D. D., Eilts, J. A., English, N. B., Weltzin, J., and Willimas,

641 D. G.: Response of net ecosystem gas exchange to a simulated precipitation pulse in a
642 semi-arid grassland: the role of native versus non-native grasses and soil texture, Oecologia,
643 141: 295-305, 2004a.
644 Huxman, T. E., Snyder, K. A., Tissue, D., Leffler, A. J., Ogle, K., Pockman, W. T., Sandquist, D.
645 R., Potts, D. L., and Schwinning, S.: Precipitation pulses and carbon fluxes in semiarid and
646 arid ecosystems, Oecologia, 141: 254-268, 2004b.
647 Huxman, T. E., Smith, M. D., Fay, P. A., Knapp, A. K., Shaw, M. R., Loik, M. E., Smith, S. D.,
648 Tissue, D. T., Zak, J. C., Weltzin, J. F., Pockman, W. T., Sala, O. E., Haddad, B. M., Harte,
649 J., Kock, G. W., Schwinning, S., Small, E. E., and Willimas, D. G.: Convergence across
650 biomes to a common rain-use efficiency, Nature, 429, 651-654, 2004c.
651 Jenerette, G. D., Barron-Gafford, G. A., Guswa, A. J., McDonnell, J. J., and Villegas, J. C.:
652 Organization of complexity in water limited ecohydrology, Ecohydrology, 5, 184-199, 2012.
653 Jenerette, G. D., Scott, R. L., and Huete, A. R.: Functional differences between summer and
654 winter season rain assessed with MODIS-derived phenology in a semi-arid region, J. Veg.
655 Sci., 21, 16-30, 2010.
656 Jenerette, G. D., Scott, R. L., and Huxman, T. E.: Whole ecosystem metabolic pulses following
657 precipitation events, Funct. Ecol., 22, 924-930, 2008.
658 Jobbagy, E. G. and Sala, O. E.: Controls of grass and shrub aboveground production in the
659 Patagonian steppe, Ecol. Appl., 10, 541-549, 2000.
660 Katul, G. A., Proporato, A., and Oren R.: Stochastic dynamics of plant-water interactions. Annu.
661 Rev. Ecol. Evol. S., 38, 767-791, 2007.

662 Kemp, P. R., Reynolds, J. F., Pachepsky, Y., and Chen, J. L.: A comparative modeling study of
663 soil water dynamics in a desert ecosystem, Water Resour. Res., 33, 73-90, 1997.
664 Kemp, P. R., Reynolds, J. F., Virginia, R. A., and Whitford, W. G.: Decomposition of leaf and
665 root litter of Chihuahuan desert shrubs: effects of three years of summer drought, J. Arid
666 Environ., 53, 21-39, 2003.
667 Knapp, A. K., Fay, P. A., Blair, J. M., Collins, S. L., Smith, M. D., Carlisle, J. D., Harper, C. W.,
668 Danner, B. T., Lett, M. S., and McCarron, J. K.: Rainfall variability, carbon cycling, and
669 plant species diversity in a mesic grassland, Science, 298, 2202-2205, 2002.
670 Lauenroth, W. K. and Sala, O. E.: Long-term forage production of North-American shortgrass
671 steppe, Ecol. Appl., 2, 397-403, 1992.
672 Ma, S. Y., Baldocchi, D. D., Hatala, J. A., Detto, M., and Yuste, J. C.: Are rain-induced
673 ecosystem respiration pulses enhanced by legacies of antecedent photodegradation in
674 semi-arid environments?, Agr. Forest Meteorol., 154, 203-213, 2012.
675 Ma, S. Y., Baldocchi, D. D., Xu, L. K., and Hehn, T.: Inter-annual variability in carbon dioxide
676 exchange of an oak/grass savanna and open grassland in California, Agr. Forest Meteorol.,
677 147, 157-171, 2007.
678 Maestre, F. T., Salguero-Gomez, R., and Quero, J. L.: It is getting hotter in here: determining and
679 projecting the impacts of global environmental change on drylands Introduction, Philos. T.
680 R. Soc. B., 367, 3062-3075, 2012.
681 McCalley, C. K., Sparks, J. P.: Abiotic gas formation drives nitrogen loss from a desert
682 ecosystem, Science, 326, 837-840, 2009.

683 McCulley, R. L., Burke, I. C., and Lauenroth, W. K.: Conservation of nitrogen increases with
684 precipitation across a major grassland gradient in the Central Great Plains of North America,
685 Oecologia, 159, 571-581, 2009.
686 Monger, C., Sala, O. E., Duniway, M. C., Goldfus, H., Meir, I. A., Poch, R. M., Throop, H. L.,
687 and Vivoni, E. R.: Legacy effects in linked ecological-soil-geomorphic systems of drylands,
688 Front. Ecol. Environ., 13, 13-19, 2015.
689 Noy-Meir, I.: Desert ecosystems: environment and producers, Annu. Rev. Ecol. Evol. S., 4,
690 25-51, 1973.
691 Oesterheld, M., Loreti, J., Semmartin, M., and Sala, O. E.: Inter-annual variation in primary
692 production of a semi-arid grassland related to previous-year production, J. Veg. Sci., 12,
693 137-142, 2001.
694 Ogle, K., Barber, J. J., Barron-Gafford, G. A., Bentley, L. P., Young, J. M., Huxman, T. E., Loik,
695 M. E., and Tissue, D. T.: Quantifying ecological memory in plant and ecosystem processes,
696 Ecol. Lett., 2014.
697 Oikawa, P. Y., Gratz, D. A., Chatterjee, A., Eberwein, J. E., Allsman, L. A., and Jenerette, G. D.:
698 Unifying soil respiration pulses, inhibition, and temperature hysteresis through dynamics of
699 labile carbon and soil O_2. J. Geophys. Res. Biogeosci., 115, 521-536, 2014.
700 Parton, W. J., Scurlock, J. M. O., Ojima, D. S., Gilmanov, T. G., Scholes, R. J., Schimel, D. S.,
701 Kirchner, T., Menaut, J. C., Seastedt, T., Moya, E. G., Kamnalrut, A., and Kinyamario, J. I.:
702 Observations and modeling of biomass and soil organic-matter dynamics for the grassland
703 biome worldwide, Global Biogeochem. Cy., 7, 785-809, 1993.

704 Paruelo, J. M., Lauenroth, W. K., Burke, I. C., and Sala, O. E.: Grassland precipitation-use
705 efficiency varies across a resource gradient, Ecosystems, 2, 64-68, 1999.
706 Peters, D. P. C., Yao, J., Sala, O. E., and Anderson, J. P.: Directional climate change and potential
707 reversal of desertification in arid and semiarid ecosystems, Global Change Biol., 18,
708 151-163, 2012.
709 Porporato, A., Daly, E., and Rodriguez-Iburbe, I.: Soil water balance and ecosystem response to
710 climate change. Am. Nat., 164, 625-632, 2004.
711 Porporato, A., and Rodriguez-Iturbe I.: Ecohydrology bearings - invited commentary from
712 random variability to ordered structures: a search for general sysnthesis in ecohydrology,
713 Ecoydrology, 6, 333-342, 2013.
714 Potts, D. L., Scott, R. L., Cable, J. M., Huxman, T. E., and Williams, D. G.: Sensitivity of
715 mesquite shrubland CO_2 exchange to precipitation in contrasting landscape settings,
716 Ecology, 89, 2900-2910, 2008.
717 Reichmann, L. G., Sala, O. E., and Peters, D. P. C.: Precipitation legacies in desert grassland
718 primary production occur through previous-year tiller density, Ecology, 94, 435-443, 2013a.
719 Reichmann, L. G., Sala, O. E., and Peters, D. P. C.: Water controls on nitrogen transformations
720 and stocks in an arid ecosystem, Ecosphere, 4, 1-17, 2013b.
721 Reynolds, J. F., Kemp, P. R., Ogle, K., and Fernandez, R. J.: Modifying the 'pulse-reserve'
722 paradigm for deserts of North America: precipitation pulses, soil water, and plant responses,
723 Oecologia, 141, 194-210, 2004.
724 Reynolds, J. F., Kemp, P. R., and Tenhunen, J. D.: Effects of long-term rainfall variability on

725 evapotranspiration and soil water distribution in the Chihuahuan Desert: A modeling
726 analysis, Plant Ecol., 150, 145-159, 2000.
727 Reynolds, J. F., Stafford Smith, D. M., Lambin, E. F., Turner, B. L., Mortimore, M., Batterbury, S.
728 P. J., Downing, T. E., Dowlatabadi, H., Fernandez, R. J., Herrick, J. E., Huber-Sannwald, E.,
729 Jiang, H., Leemans, R., Lynam, T., Maestre, F. T., Ayarza, M., and Walker, B.: Global
730 desertification: Building a science for dryland development, Science, 316, 847-851, 2007.
731 Reynolds, J. F., Virginia, R. A., Kemp, P. R., de Soyza, A. G., and Tremmel, D. C.: Impact of
732 drought on desert shrubs: Effects of seasonality and degree of resource island development,
733 Ecol. Monogr., 69, 69-106, 1999.
734 Reynolds, J. F., Virginia, R. A., and Schlesinger, W. H.: Defining functional types for models of
735 desertification. In: Plant Functional Types: Their Relevance to Ecosystem Properties and
736 Global Change, Shugart, T. M. and Woodward, F. I. (Eds.), Cambridge University Press,
737 Cambridge, 1997.
738 Rodriguez-Iturbe, I., Isham, V., Cox D. R., Manfreda, S., and Porporato A.: Space-time modeling
739 of soil moisture: Stochastic rainfall forcing with heterogeneous vegeation. Water Resour.
740 Res., 42, doi: 10.1029/2005WR004497, 2006.
741 Sala, O. E., Gherardi, L. A., Reichmann, L., Jobbagy, E., and Peters, D.: Legacies of
742 precipitation fluctuations on primary production: theory and data synthesis, Philos. T. R.
743 Soc. B., 367, 3135-3144, 2012.
744 Sala, O. E., Lauenroth, W. K., and Parton, W. J.: Long-term soil-water dynamics in the shortgrass
745 steppe, Ecology, 73, 1175-1181, 1992.

746 Schlesinger, W. H.: Biogeochemistry: An Analysis of Global Change, Academic Press Inc, San
747 Diego, CA. , 1991.
748 Scott, R. L., Hamerlynck, E. P., Jenerette, G. D., Moran, M. S., and Barron-Gafford, G. A.:
749 Carbon dioxide exchange in a semidesert grassland through drought-induced vegetation
750 change, J. Geophys. Res. Biogeosci., 115, G03026, doi: 03010.01029/02010JG001348,
751 2010.
752 Scott, R. L., Huxman, T. E., Barron-Gafford, G. A., Jenerette, G. D., Young, J. M., and
753 Hamerlynck, E. P.: When vegetation change alters ecosystem water availability, Global
754 Change Biol., 20, 2198-2210, 2014.
755 Scott, R. L., Jenerette, G. D., Potts, D. L., and Huxman, T. E.: Effects of seasonal drought on net
756 carbon dioxide exchange from a woody-plant-encroached semiarid grassland, J. Geophys.
757 Res. Biogeosci., 114, G04004, doi: 04010.01029/02008JG000900, 2009.
758 Seager, R., Ting, M. F., Held, I., Kushnir, Y., Lu, J., Vecchi, G., Huang, H. P., Harnik, N.,
759 Leetmaa, A., Lau, N. C., Li, C. H., Velez, J., and Naik, N.: Model projections of an
760 imminent transition to a more arid climate in southwestern North America, Science, 316,
761 1181-1184, 2007.
762 Shen, W. J., Jenerette, G. D., Hui, D. F., Phillips, R. P., and Ren, H.: Effects of changing
763 precipitation regimes on dryland soil respiration and C pool dynamics at rainfall event,
764 seasonal and interannual scales, J. Geophys. Res. Biogeosci., 113, G03024, doi:
765 03010.01029/02008JG000685, 2008a.
766 Shen, W. J., Reynolds, J. F., and Hui, D. F.: Responses of dryland soil respiration and soil carbon

767 pool size to abrupt vs. gradual and individual vs. combined changes in soil temperature,
768 precipitation, and atmospheric [CO_2]: a simulation analysis, Global Change Biol., 15,
769 2274-2294, 2009.
770 Shen, W. J., Wu, J. G., Grimm, N. B., and Hope, D.: Effects of urbanization-induced
771 environmental changes on ecosystem functioning in the Phoenix metropolitan region, USA,
772 Ecosystems, 11, 138-155, 2008b.
773 Shen, W. J., Wu, J. G., Kemp, P. R., Reynolds, J. F., and Grimm, N. B.: Simulating the dynamics
774 of primary productivity of a Sonoran ecosystem: Model parameterization and validation,
775 Ecol. Model., 189, 1-24, 2005.
776 Sherry, R. A., Weng, E. S., Arnone, J. A., Johnson, D. W., Schimel, D. S., Verburg, P. S., Wallace,
777 L. L., and Luo, Y. Q.: Lagged effects of experimental warming and doubled precipitation on
778 annual and seasonal aboveground biomass production in a tallgrass prairie, Global Change
779 Biol., 14, 2923-2936, 2008.
780 Solomon, S., Qin, D., Manning, M., Chen, Z., Marquis, M., Averyt, K. B., Tignor, M., and Miller,
781 H. L. (Eds.): Climate Change 2007: The Physical Science Basis, Cambridge University
782 Press, Cambridge, 2007.
783 Sponseller, R. A.: Precipitation pulses and soil CO_2 flux in a Sonoran Desert ecosystem, Global
784 Change Biol., 13, 426-436, 2007.
785 Swemmer, A. M., Knapp, A. K., and Snyman, H. A.: Intra-seasonal precipitation patterns and
786 above-ground productivity in three perennial grasslands, J. Ecol., 95, 780-788, 2007.
787 Vargas, R., Baldocchi, D. D., Allen, M. F., Bahn, M., Black, T. A., Collins, S. L., Yuste, J. C.,

788 Hirano, T., Jassal, R. S., Pumpanen, J., and Tang, J. W.: Looking deeper into the soil:
789 biophysical controls and seasonal lags of soil CO_2 production and efflux, Ecol. Appl., 20,
790 1569-1582, 2010.
791 Wiegand, T., Snyman, H. A., Kellner, K., and Paruelo, J. M.: Do grasslands have a memory:
792 Modeling phytomass production of a semiarid South African grassland, Ecosystems, 7,
793 243-258, 2004.
794 Willimas, C. A. and Albertson, J. D.: Dynamical effects of the statistical structure of annual
795 rainfall on dryland vegetation, Global Change Biol., 12, 777-792, 2006.
796 Williams, C. A., Hanan, N., Scholes, R. J., and Kutsch, W.: Complexity in water and carbon
797 dioxide fluxes following rain pulses in an african savanna, Oecologia, 161, 469-480, 2009.
798 Xu, L. K. and Baldocchi, D. D.: Seasonal variation in carbon dioxide exchange over a
799 Mediterranean annual grassland in California, Agr. Forest Meteorol., 123, 79-96, 2004.
800 Xu, L. K., Baldocchi, D. D., and Tang, J. W.: How soil moisture, rain pulses, and growth alter the
801 response of ecosystem respiration to temperature, Global Biogeochem. Cy., 18, GB4002,
802 doi: 4010.1029/2004GB002281, 2004.
803 Yahdjian, L. and Sala, O. E.: Vegetation structure constrains primary production response to
804 water availability in the Patagonian steppe, Ecology, 87, 952-962, 2006.
805 Yahdjian, L., Sala, O. E., and Austin, A. T.: Differential controls of water input on litter
806 decomposition and nitrogen dynamics in the Patagonian Steppe, Ecosystems, 9, 128-141,
807 2006.
808 Yahdjian, L., Sala, O. E.: Size of precipitatin pulses controls nitrogen transformation and losses

809 in an arid Patagonian ecosystem, Ecosystems, 13, 575-585, 2010.
810 Zielis, S., Etzold, S., Zweifel, R., Eugster, W., Haeni, M., and Buchmann, N.: NEP of a Swiss
811 subalpine forest is significantly driven not only by current but also by previous year's
812 weather, Biogeosciences, 11, 1627-1635, 2014.
813
814

815 **Table 1.** Spearman correlation coefficients between interannual legacy effects and precipitation
816 characteristics. Significant correlations are indicated with * for 0.01<P≤0.05 and ** for P≤
817 0.01 (2-tailed; n=27).

Precipitation	Dry legacy (previous-year PPT -30%)			Wet legacy (previous-year PPT +30%)		
characteristics	ΔGEP	ΔR_e	ΔNEP	ΔGEP	ΔR_e	ΔNEP
Previous-year PPT characteristics						
Yearly rainfall	0.134	0.033	0.0.270	-0.324	-0.180	-0.374
Warm-GS rainfall	0.303	0.072	0.519**	-0.430*	-0.065	-0.579**
Warm-GS BEI	-0.069	0.137	-0.399*	-0.075	0.053	-0.262
Warm-GS NE>10 mm	0.329	0.067	0.636**	-0.535**	-0.227	-0.619**
Current-year PPT characteristics						
Yearly rainfall	0.278	0.162	0.484*	-0.466*	-0.600**	-0.224
Cool-GS rainfall	0.528**	0.338	0.495*	-0.277	-0.331	-0.218
Yearly BEI	-0.512**	-0.285	-0.686**	0.359	0.352	0.255
Cool-GS BEI	-0.519**	-0.286	-0.510**	0.151	0.088	0.214
Yearly NE>10 mm	0.331	0.178	0.512**	-0.567**	-0.583*	-0.398*
Cool-GS NE<10 mm	0.614**	0.577**	0.398*	-0.105	-0.075	-0.128
PPT difference (ΔPPT) between current- and previous-year						
Yearly rainfall	0.088	-0.135	0.466*	0.078	-0.088	0.252
Warm-GS rainfall	-0.059	-0.042	0.074	0.206	-0.096	0.326

Cool-GS rainfall	0.326	0.048	0.374*	0.248	0.160	0.209

Abbreviations: PPT: precipitation; GEP: gross primary production; R_e: ecosystem respiration; NEP: net ecosystem production; GS: growing season; BEI: between-event interval; NE: number of rainfall events.

821 **Figure captions**

822 **Figure 1.** Precipitation characteristics in the 30 years (1981-2010) at the Santa Rita mesquite
823 savanna site. (a) Annual and seasonal precipitation amount; (b) Frequency distribution of daily
824 rainfall; (c) Mean and maximum between-event interval (BEI). Horizontal lines within (a)
825 indicate mean annual and seasonal precipitation. The warm growing season (warm-GS) is from
826 Jul through Sep, the cool dry season (cool-DS) from Oct to Nov, the cool growing season
827 (cool-GS) from Dec through Mar, and the warm dry season (warm-DS) from Apr through Jun.
828 Error bars in panel (c) represent standard deviations and n is the number of rain event pairs used
829 to calculate the between-event interval in the 30 years.

830

831 **Figure 2.** Comparison of the model-simulated water and carbon fluxes with the eddy
832 covariance observations at the mesquite savanna site. Left panels show the comparison
833 between the modeled and observed fluxes in four calibration (2007-2007; solid dots) and three
834 validation years (2008-2010; open dots). Right panels show the relationships of the simulated
835 (solid dots) and observed (open dots) fluxes with precipitation in the seven years (2004-2010).
836 R^2 is the coefficient of determination describing the proportion of the variance in measured
837 fluxes explained by the model for the left panels or that explained by precipitation for the right
838 panels. AET represents actual evapotranspiration; GEP gross ecosystem production, R_e total
839 ecosystem respiration, and NEP net ecosystem production.

840

841 **Figure 3.** Interdecadal legacy effects of changing the previous-period (1981-1994)

842 precipitation on the cumulative carbon fluxes of the current period (1995-2010). Interdecadal
843 legacy effects on carbon fluxes (e.g. ΔNEP) are calculated as the difference between the
844 current-period flux with previous-period PPT changes and that without previous-period PPT
845 changes. Dashed lines with open symbols represent different levels of decreasing the
846 current-period precipitation (left panels). Solid lines with filled symbols represent increasing
847 the current-period precipitation (right panels).
848
849 **Figure 4.** Spearman correlations of interdecadal precipitation legacy effects with the
850 precipitation difference between periods (ΔPPT). Interdecadal ΔPPT is calculated as the mean
851 PPT of the current period (1995-2010) minus that of the previous period (1981-1994).
852 Interdecadal legacy effects on carbon fluxes (e.g. ΔNEP) are calculated as the difference
853 between the current-period flux with previous-period PPT changes and that without
854 previous-period PPT changes. Sample size is 41 for the wet-to-dry period transition (left panels)
855 and 23 for the dry-to-wet period transition (right panels). GEP represents gross ecosystem
856 production, R_e ecosystem respiration, and NEP net ecosystem production. R^2 is the coefficient
857 of determination and P is probability.
858
859 **Figure 5.** Interdecadal precipitation legacy effects on the resource pool dynamics. Left
860 panels show the resource pool responses under a 30% of decrease while right panels show those
861 under a 30% of increase in the precipitation (PPT) of the current period from 1995-2010.

862 Legacy effects on pool size (e.g. ΔBiomass) are quantified as the difference between the
863 current-period pool size with previous-period PPT change and that without previous-period PPT
864 change. Dashed lines represent a 30% of decrease while solid lines represent a 30% of increase
865 in the PPT of the previous period from 1981-1994. SOM represents soil organic matter, N_{soil}
866 soil mineral nitrogen, and SWC soil water content.
867
868 **Figure 6.** Interannual precipitation legacy effects on the ecosystem carbon fluxes. (a) and (b)
869 show the lasting duration of dry (left panels) and wet (right panels) legacies, respectively. The
870 legacy lasting duration is quantified as the number of years during which the legacy impacts on
871 ecosystem fluxes exists after a previous-year PPT change. (c) through (h) show the responses
872 of gross ecosystem production (GEP), ecosystem respiration (R_e) and net ecosystem production
873 (NEP) to dry (left panels) and wet (right panels) legacies. Bars in the background of (a) and (b)
874 represent the previous-year PPT amount after a 30% decrease and increase, respectively.
875
876 **Figure 7**. Interannual precipitation legacy effects on resource pool dynamics. Left panels
877 show the legacy effects on pool dynamics in two representative wet years while right panels for
878 two representative dry years. Legacy effects on pool size (e.g. ΔBiomass) are quantified as the
879 difference between the current-year pool size with previous-year PPT change and that without
880 previous-year PPT change. Solid lines represent a 30% decrease while dashed lines represent a
881 30% increase in the previous-year precipitation (PPT). SOM represents soil organic matter,
882 N_{soil} soil mineral nitrogen, and SWC soil water content.

883

884 FIG. 1

885

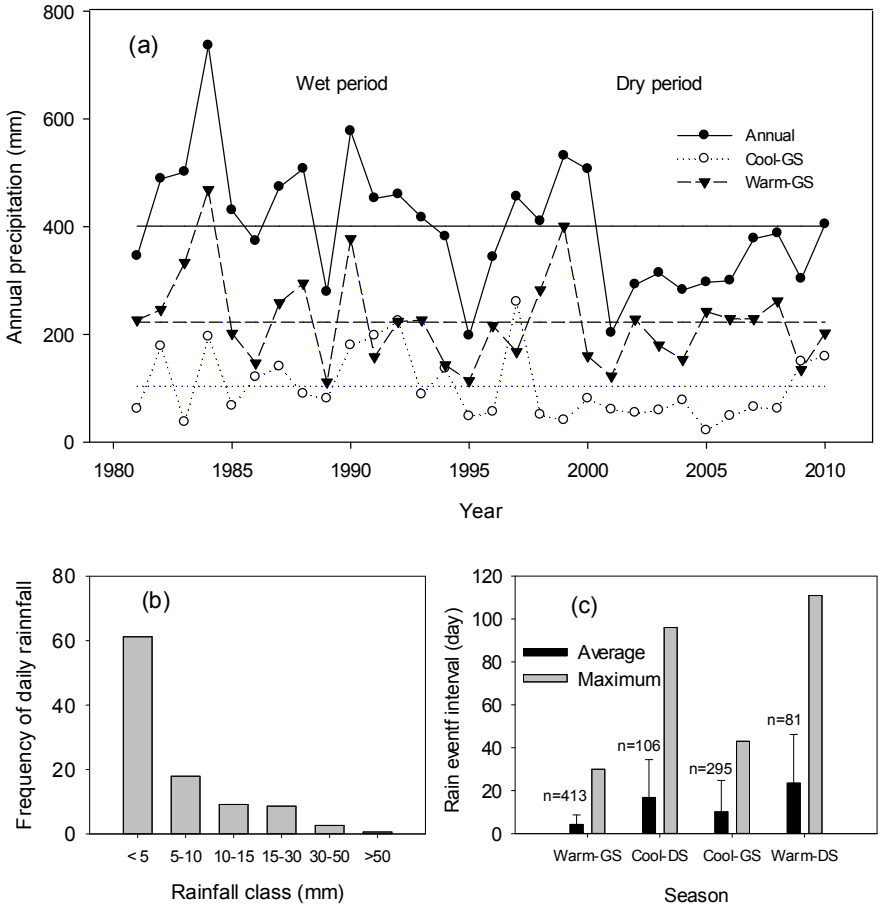

886

887

888

889 FIG. 2
890

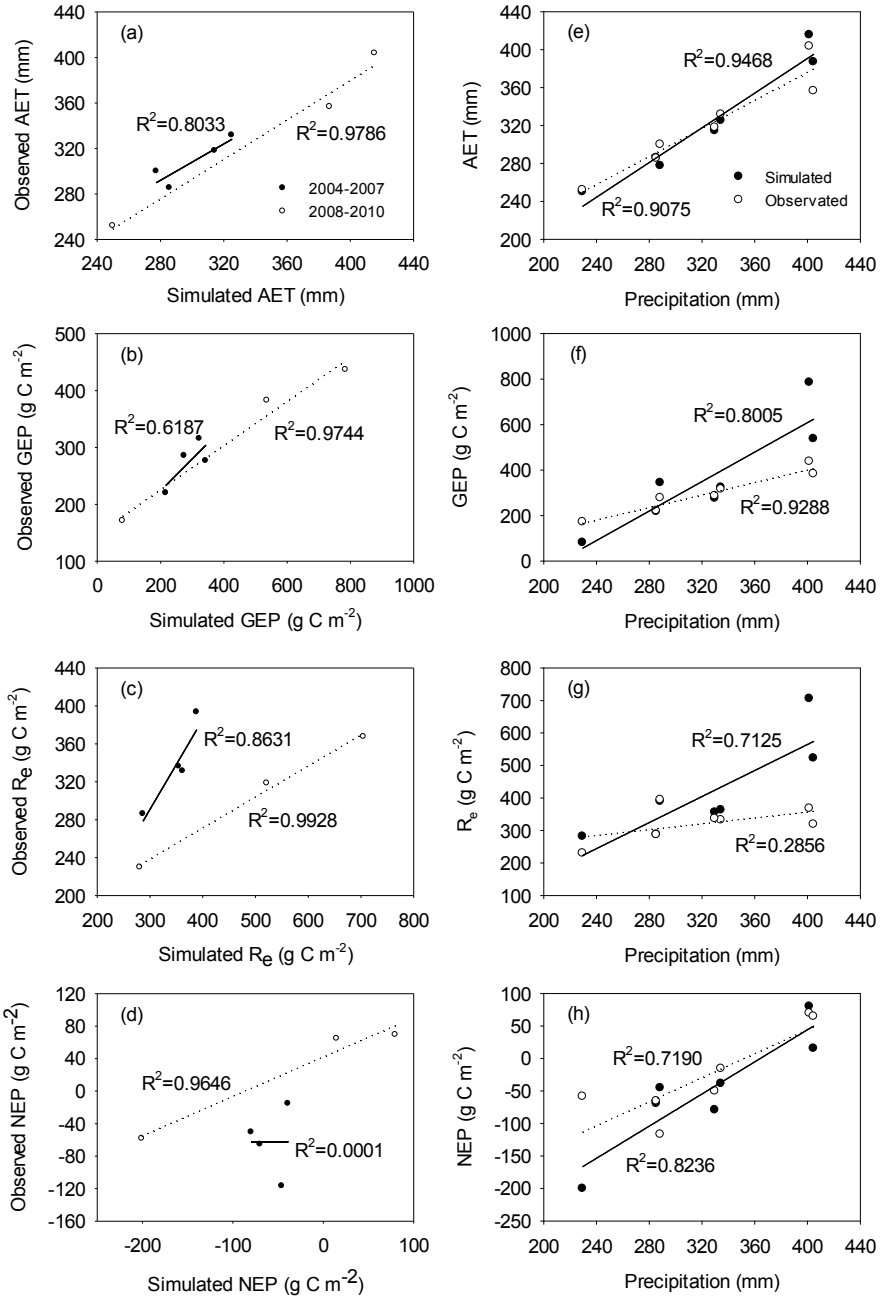

891
892

893

894 FIG. 3

895

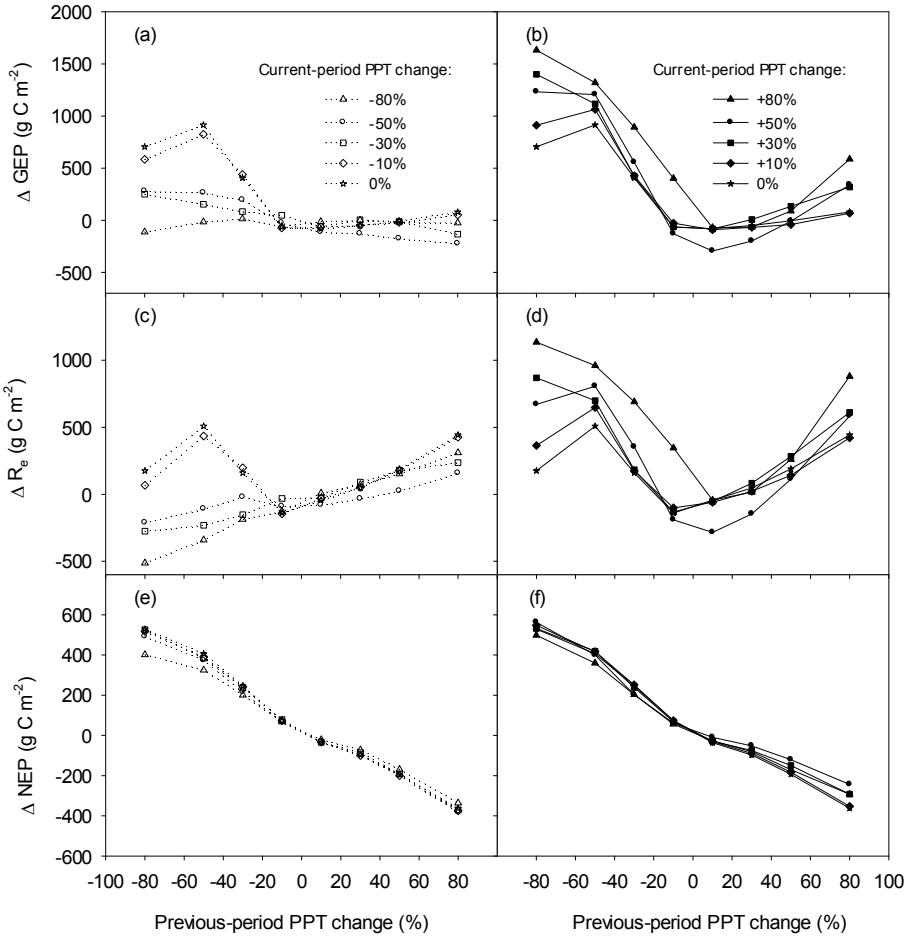

896

897

898

899 FIG. 4

900

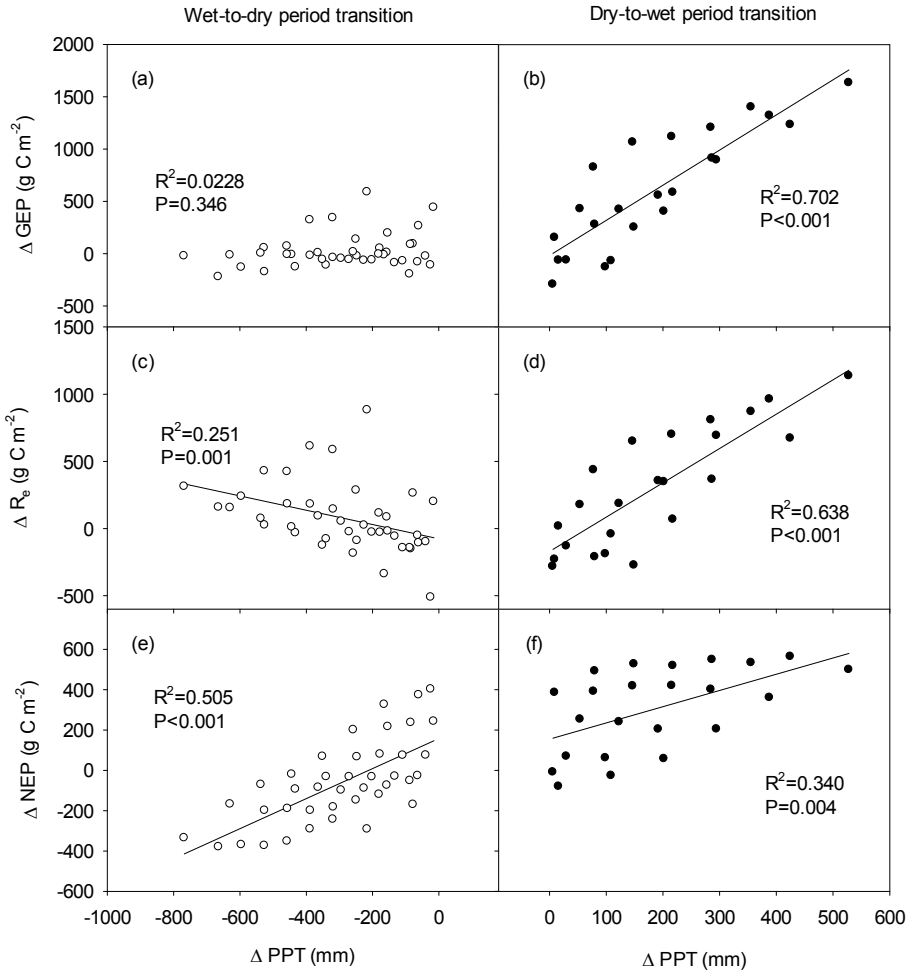

901

902

903

904 FIG. 5

905

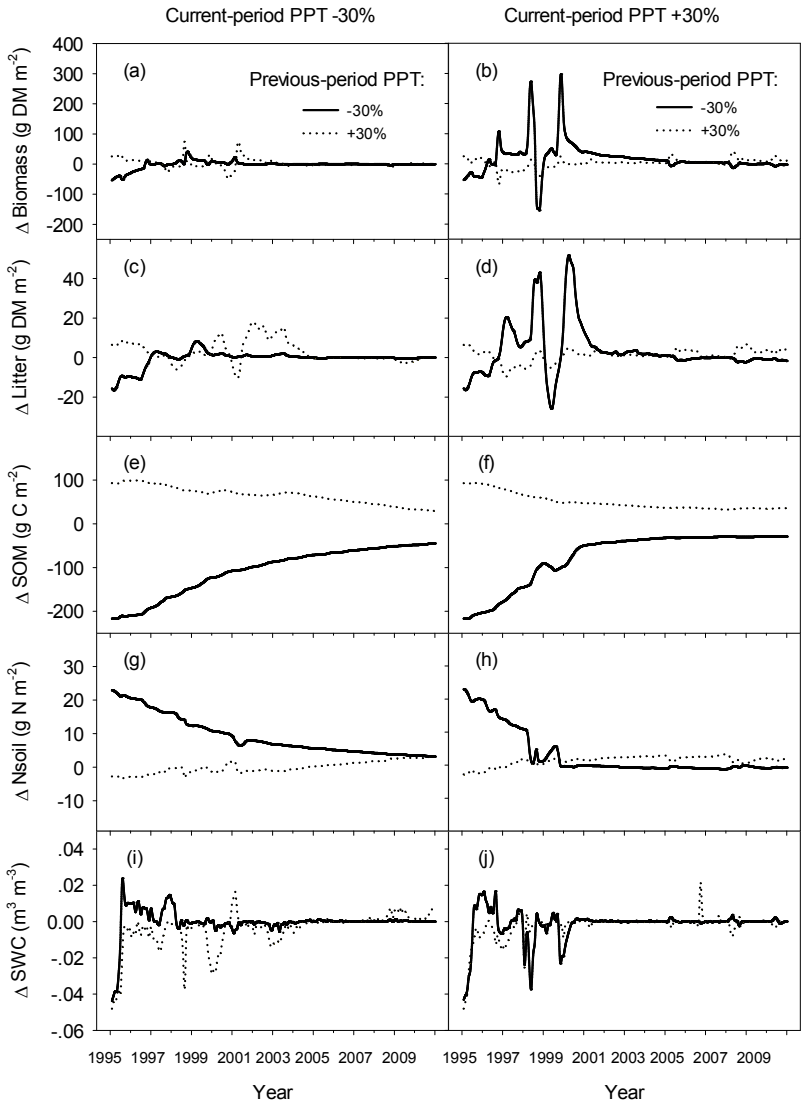

906

907

908

909 FIG. 6

910

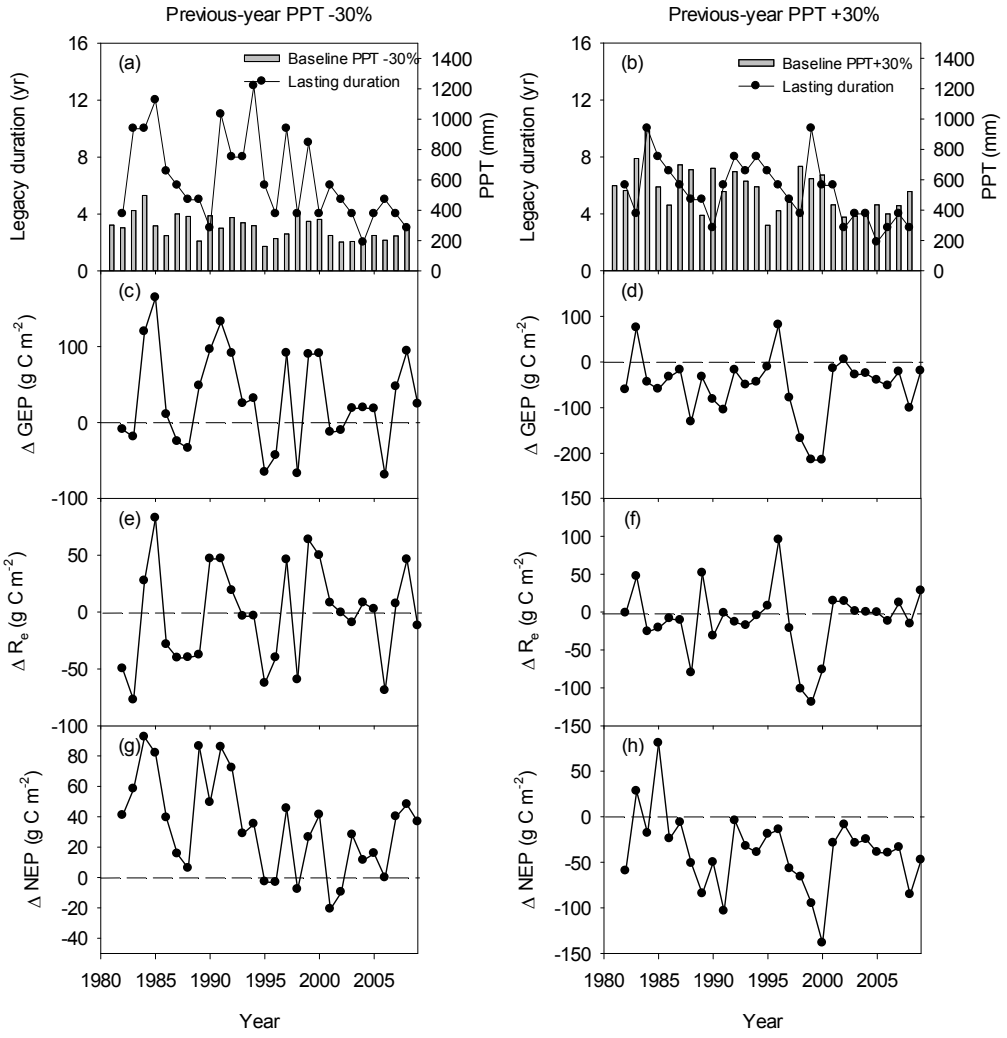

911

912

913

914

915

916

917 FIG. 7

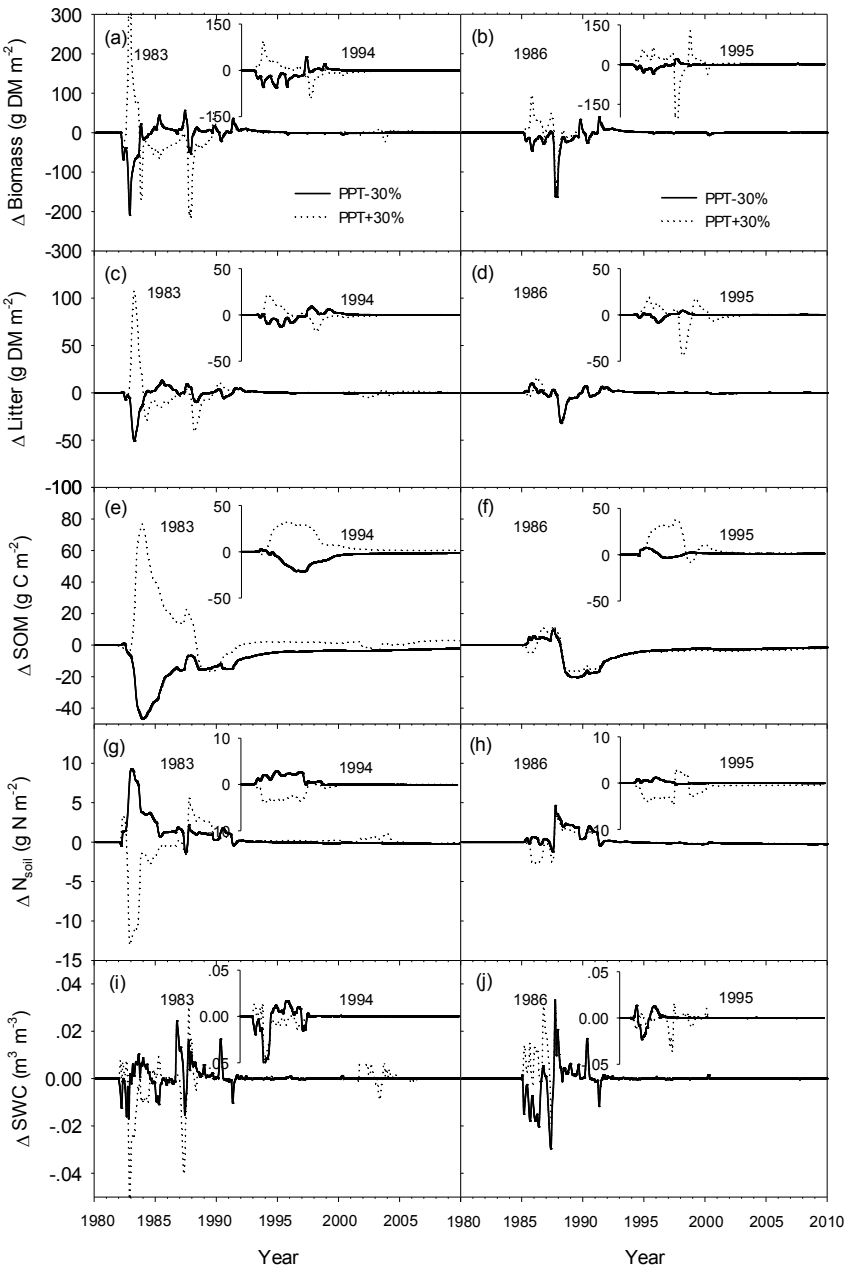

918